

PAPER • OPEN ACCESS

Overview of tritium retention in divertor tiles and dust particles from the JET tokamak with the ITER-like wall






To cite this article: Y. Torikai *et al* 2024 *Nucl. Fusion* **64** 016032

View the [article online](#) for updates and enhancements.

You may also like

- [An overview of tritium retention in dust particles from the JET-ILW divertor](#)
T Otsuka, S Masuzaki, N Ashikawa et al.
- [Experience on divertor fuel retention after two ITER-Like Wall campaigns](#)
K Heinola, A Widdowson, J Likonen et al.
- [Overview of fuel inventory in JET with the ITER-like wall](#)
A. Widdowson, J.P. Coad, E. Alves et al.

Overview of tritium retention in divertor tiles and dust particles from the JET tokamak with the ITER-like wall

Y. Torikai^{1,*}, G. Kikuchi¹, A. Owada¹, S. Masuzaki² , T. Otsuka³, N. Ashikawa^{2,4}, M. Yajima², M. Tokitani² , Y. Oya⁵, S.E. Lee⁶, Y. Hatano⁶ , N. Asakura⁷, T. Hayashi⁸, M. Oyaidzu⁸, J. Likonen⁹, A. Widdowson¹⁰ , M. Rubel^{11,12}  and JET Contributors¹³

¹ Ibaraki University Graduate School of Science and Engineering, Mito, Japan

² National Institute for Fusion Science, Toki, Japan

³ Kindai University, Higashi-Osaka, Japan

⁴ SOKENDAI, Toki, Japan

⁵ Shizuoka University, Shizuoka, Japan

⁶ Hydrogen Isotope Research Center, University of Toyama, Toyama, Japan

⁷ National Institute for Quantum and Radiological Science and Technology, Naka, Japan

⁸ National Institute for Quantum and Radiological Science and Technology, Rokkasho, Japan

⁹ VTT Technical Research Centre of Finland, Otakaari 3J, 02150 Espoo, Finland

¹⁰ Culham Centre for Fusion Energy, United Kingdom Atomic Energy Authority, Culham Science Center, Abingdon OX14 3DB, United Kingdom of Great Britain and Northern Ireland

¹¹ KTH Royal Institute of Technology, 100 44 Stockholm, Sweden

¹² Uppsala University, Box 516, 751 20 Uppsala, Sweden

E-mail: yuji.torikai.sci@vc.ibaraki.ac.jp

Received 5 May 2023, revised 6 September 2023

Accepted for publication 13 November 2023

Published 5 December 2023



Abstract

Divertor tiles after Joint European Torus-ITER like wall (JET-ILW) campaigns and dust collected after JET-C and JET-ILW operation were examined by a set of complementary techniques (full combustion and radiography) to determine the total, specific and areal tritium activities, poloidal tritium distribution in the divertor and the presence of that isotope in individual dust particles. In the divertor tiles, the majority of tritium is detected in the surface region and, the areal activities in the ILW divertor are in the 0.5–12 kBq cm⁻² range. The activity in the ILW dust is associated mainly with the presence of carbon particles being a legacy from the JET-C operation. The total tritium activities show significant differences between the JET operation with ILW and the earlier phase with the carbon wall (JET-C) indicating that tritium retention has been significantly decreased in the operation with ILW.

Keywords: JET, ITER like wall, tritium, divertor, dust

(Some figures may appear in colour only in the online journal)

¹³ See Mailloux *et al* 2022 (<https://doi.org/10.1088/1741-4326/ac47b4>) for JET Contributors.

* Author to whom any correspondence should be addressed.



Original content from this work may be used under the terms of the [Creative Commons Attribution 4.0 licence](https://creativecommons.org/licenses/by/4.0/). Any further distribution of this work must maintain attribution to the author(s) and the title of the work, journal citation and DOI.

1. Introduction

Joint European Torus (JET) has been operated since August 2011 with metallic plasma-facing components (PFCs): JET-ITER like wall (JET-ILW) with beryllium (Be) limiters in the main chamber and tungsten (W) in the divertor [1]. Successful operation with the metal wall had a major impact on the decision regarding materials for PFC in ITER: to eliminate carbon tiles in the divertor, and to start from day 1 with Be and W components [2]. PFC tiles and dust particles retrieved from JET-ILW are at the centre of comprehensive research carried out since 2014 in European laboratories and in the framework of the Procurement Agreement of the Broader Approach signed by Japan (JA) and EU. The emphasis in the cooperation is on further progress in fusion science and technology, in particular tritium (T) technology: T analysis methods (understanding and development) and accountancy in reactor materials, and detailed PFC characterisation.

The operation of JET-ILW was preceded by 25 years (1984–2009) of experimental campaigns in JET with carbon PFC, referred to as JET-C. All aspects regarding subsequent phases (including a full deuterium–tritium campaign in 1997) and their impact on PFC morphology and fuel retention are detailed in [3], while a complete technological and scientific motivation for the transition to the metal wall is in [1]. It should also be stressed that both JET-C and JET-ILW plasma discharges were fuelled with deuterium thus generating some quantities of tritium through one branch of the D–D reactions. Therefore, the campaigns in JET-ILW facilitate detailed studies of fuel retention, erosion–deposition processes and dust generation under conditions relevant for a reactor-class device, i.e. ITER. They also enable comprehensive comparison between JET-C and JET-ILW in the area plasma–wall interactions.

Until year 2016 three JET-ILW campaigns have been fully completed: ILW-1 (2011–2012, input energy of 150 GJ), ILW-2 (2013–2014, energy 201 GJ) and ILW-3 (2015–2016, energy 245 GJ) [4]. A significant number of samples from wall tiles and dust (both from ILW-1 and ILW-3) as well as dust from JET-C were shipped from JET to the International Fusion Energy Research Center of QST, Rokkasho, JA. The study reported below comprised a number of objectives: (i) to determine T content in the tiles and in dust particles retrieved after the ILW-1 and ILW-3; (ii) to quantify that isotope in dust collected from JET-C; (iii) to draw conclusions arising from comparisons of material properties following the operation campaigns; (iv) to identify possible sources of errors and discrepancies.

2. Experimental

The study was carried out on two types of samples: (a) JET-ILW divertor tiles W-coated carbon-fibre composites (W/CFCs) after ILW-1 and ILW-3 campaigns; (b) samples

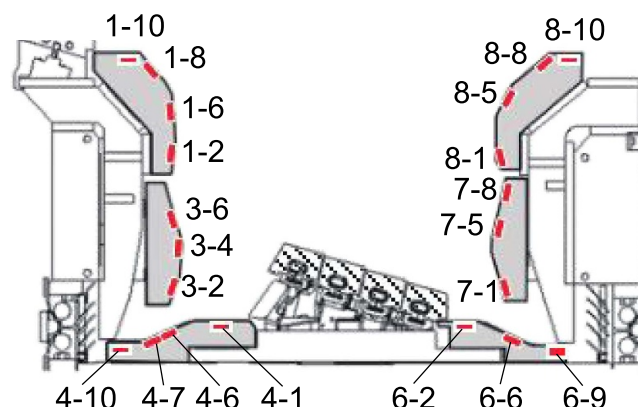


Figure 1. Cross-section of the JET-ILW divertor with marked position of the samples.

of dust retrieved after the operation in JET-C and then in ILW-1 and ILW-3. The tiles selected for studies were sectioned (cut) to obtain samples which could be handled in respective analytical systems. Tritium analyses were performed by means of radiography using a tritium imaging plate technique (TIPT) [5, 6], full combustion method (FCM) [7] and liquid scintillation counter (LSC). The identification of individual dust particles was done using scanning electron microscopy (SEM) and electron microprobe analyser [8].

2.1. Specimens

2.1.1. Dust. Dust particles removed from the vacuum vessel by a cyclone-type vacuum cleaner after three different experimental phases in JET have been studied: JET-C operation in 2007–2009, ILW-1 and ILW-3. Particles in JET-C were collected from six positions: inner divertor tiles, divertor carrier ribs, outer divertor base tiles, water-cooled louvres in the remote region (pumping duct) of the inner and outer divertor [9]. After the ILW campaigns dust was collected from the inner (tiles 0, 1, 3 and 4) and outer (tiles 5, 6, 7 and 8) divertor tiles [2]; tile 0 acts as a high field gap closure. In total 280 g was collected in JET-C, while the amount of dust generated in the presence of metal wall was very small: around 1 g per ILW campaign [4, 10]. Dust particles from each location were stored in separate glass pots.

2.1.2. Divertor tiles. Two sets of 21 samples each were studied. The cross-section of the JET-ILW divertor with marked positions of the samples is shown in figure 1. The notation (e.g. 1–10) denotes tile—sample numbers. Images in figures 2(a)–(d) show respectively: (a) tile 4 as retrieved after ILW-1, (b) the same tile after preparation of specimens by coring, (c) the cored disc and, (d) a triangular sample (approximately 2 mm long edges and 0.5–2 mm thickness) cut-out from that disc for tritium studies by FCM.

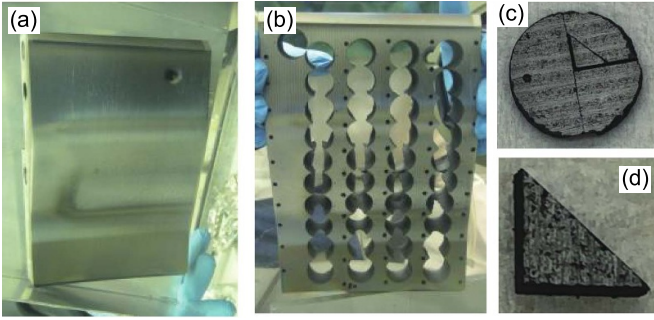


Figure 2. Photographs of ILW-1 divertor tile 4 and samples prepared for FCM: (a) divertor tile, (b) cored tile, (c) cored samples and (d) sample machined for tritium analysis by FCM.

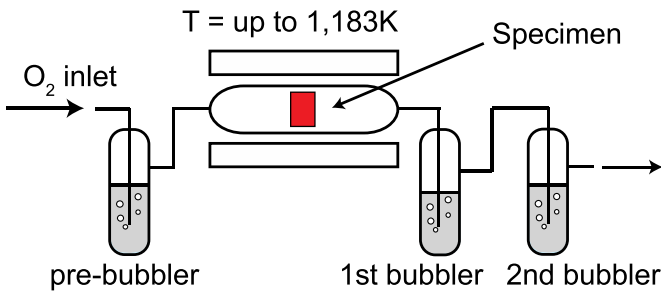


Figure 3. Experimental set-up for tritium measurement using the full combustion method.

2.2. Enhanced FCM

FCM is a standard technique of tritium analysis to determine the total amount of T retained in materials [11]. To measure effectively T removal from dust and PFC tiles, a modified FCM approach was applied. The experimental set-up is shown in figure 3. A special feature was the use a tin (Sn) foil for wrapping specimens of dust and tiles for combustion in the flowing oxygen used both as a carrier gas and the oxidising agent. Such small packages were then placed on a ceramic plate in a quartz tube inserted to a ceramic furnace. The package was heated up to 1200 K with a heating rate of 85 K min^{-1} and kept at that temperature for 30 min. At the temperature of 1100–1200 K Sn reacts chemically with oxygen (oxidises) and the temperature rises to about 2100 K [12]. Consequently, the Sn foil and specimens are combusted and turned into ash remaining on the ceramic plate. The released tritium in the form of tritiated water (HTO) was trapped in two water-filled bubblers placed in a series downstream of the quartz tube. The role of a water bubbler installed before the tube oven was to humidify oxygen flowing to the heated sample. After switching-off the oven and cooling down the quartz tube, the two downstream bubblers were disconnected, and the released tritium was measured using LSC. In order to measure T remaining in the quartz tube after heating, another water-filled bubbler was connected downstream of the quartz tube in the place of bubblers 1 and 2, and oxygen was passed through the reactor tube for 30 min. The third bubbler was

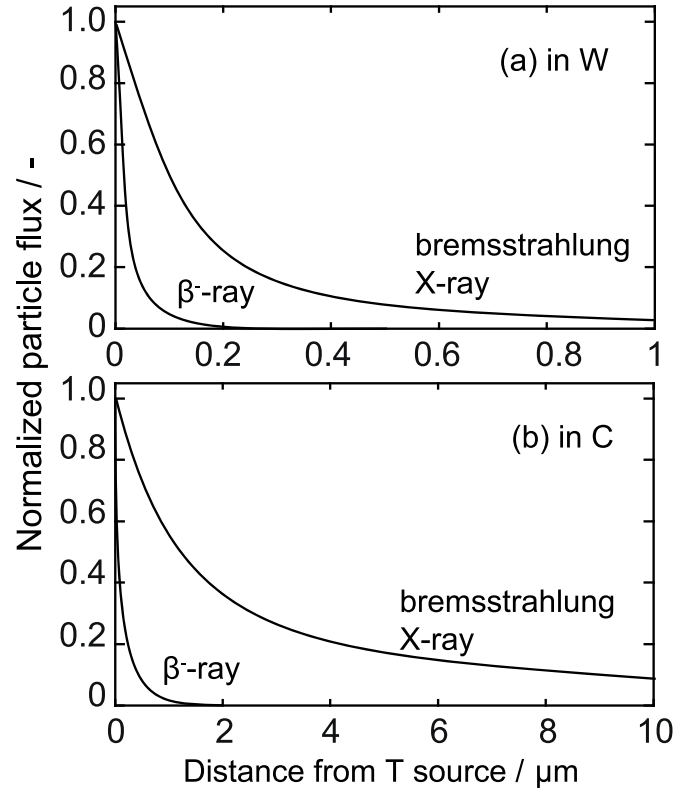


Figure 4. Intensity of normalised particle flux dependent on transmission distance of β^- -rays and Bremsstrahlung x-rays for tritium in (a) W and (b) C targets calculated by the Monte Carlo method PHITS.

then disconnected, and tritium was measured by LSC. The ash located on the ceramic plate was also put into the scintillation cocktail to determine the remaining amount of that isotope.

The normalisation of the FCM tritium data is presented in terms of specific tritium activity (kBq g^{-1}) $A_{\text{sp}}(\text{T})$ and areal tritium $A_{\text{a}}(\text{T})$ (kBq cm^{-2}) depending on the samples discussed.

2.3. Measurements with TIPT

Figure 4 shows the attenuation of the β^- particles and x-rays intensity with depth in W and C, as calculated by Monte Carlo particle transport simulation code ‘Features of Particle and Heavy Ion Transport Code System (PHITS)’ [13]. In the PHITS simulation of the β^- -ray range, the DECDC76 nuclear decay database (equivalent to ICRP107) is used to obtain the energy of tritium β^- -ray spectra. The horizontal axis shows the distance from the source of T, and the vertical axis shows the intensity of the particle flux. The range of β^- is very short: the decrease to 1% in W is within $0.167 \mu\text{m}$, and even in C it is only $1.2 \mu\text{m}$. The range of bremsstrahlung x-ray induced by T is longer than that of β^- -rays, and the distance of decay to 1% in W is $2 \mu\text{m}$, while in C it is $64 \mu\text{m}$. TIPT can then trace T present on the surface region of those depths. Table 1 summarises the attenuation of the particle flux and the transmission distance. TIPT(X) is superior to TIPT(β^-) for measuring the

Table 1. Relation between particle transmission distance and transmittance calculated by the Monte Carlo method.

Transmission distance from the source where the particle flux decreases to	β^- -ray in W μm^{-1}	Bremsstrahlung x-ray in W μm^{-1}	β^- -ray in C μm^{-1}	Bremsstrahlung x-ray in C μm^{-1}
50%	0.012	0.085	0.049	1.31
10%	0.067	0.411	0.42	11.4
1%	0.167	2.07	1.21	136
0.1%	0.269	6.39	1.96	— ^a
0.01%	0.366	12.7	2.58	— ^a

^a The escape depth is so deep that it cannot be calculated with the same precision as other calculations.

distribution of T produced by the DD reaction. The conversion efficiency from β^- -rays to bremsstrahlung is only 0.4%, thus indicating that the TIPT(β^-) method is sensitive.

Two types of imaging plates (IPs) were used. One is BAS-TR type (Fujifilm, Japan). This type of IP has 50 μm -thick phosphor coating without any protection layer and sensitive to low energy (≤ 18.6 keV) β^- -rays from T. The other is BAS-MS type (Fujifilm, Japan) having 115 μm -thick phosphor layers covered by 9 μm -thick plastic layer for protection of hygroscopic phosphor. The latter was used to examine the intensity of x-rays induced by β^- -rays from T. In contrast to BAS-TR, BAS-MS is insensitive to β^- -rays from T because the β^- -rays are fully attenuated in the plastic protection layer. From the equation proposed by Katz and Penfold (equation (8) in [14]), the escape depths of β^- -rays in W, Be and BeO were evaluated to be 0.3, 3 and 2 μm , respectively. The x-ray spectra induced by β^- -rays cover the energy range up to 10 keV. From the mass attenuation coefficients for W, Be and O, the escape depth of 5 keV x-rays was evaluated to be 2 μm in W, 2800 μm in Be and 280 μm in BeO. Here, the escape depth is defined as material thickness by which the intensity of x-rays is attenuated to 1/10. The β^- -rays IP (BAS-TR) is suitable to evaluate distributions of T on/near the surface of tiles such as T retained in the co-deposits. The x-ray IP was used to study the distribution of T retained in the deeper regions of the tiles.

2.4. Tritium measurement in dust by TIPT combined with SEM/EPMA

A tiny amount of dust was taken from the pot and gently placed on the surface of an indium (In) disc. The advantage of using such substrate is a negligible intensity of background carbon, while most types of adhesive tapes used to attach samples for analysis include carbon [15]. Tritium retained in the dust particles was assessed by TIPT with the spatial resolution of 25 μm [16, 17]. The emission of β^- -rays from T to the IP was measured over the whole surface of the In disc for 1 h at room temperature. Afterwards scanning electron microscope (SEM) and electron probe micro analyzer (EPMA) were conducted to determine morphology (composition and structure) of particles on the same surface area where the TIPT was used. EPMA with a 10 keV electron beam gives information on the elemental composition with a spatial resolution of around 1 μm . Individual dust particles were separately analysed. Maps (images) of T distribution and elemental composition were

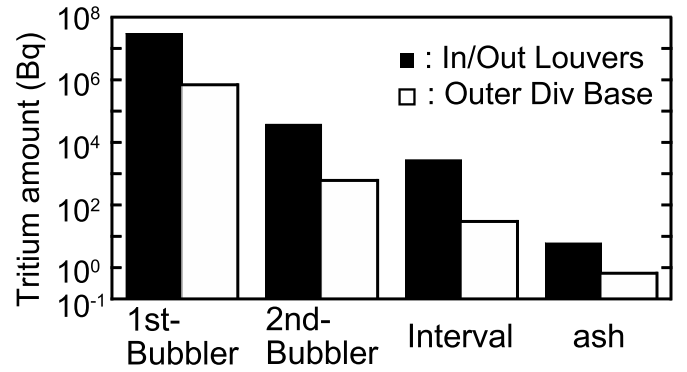


Figure 5. T contents in dust from the louvres and the outer divertor base in JET-C measured by FCM.

super-imposed to reveal characteristic features of T retention in the individual particles. Software FIZI was used for image analysis [18].

3. Results

3.1. Tritium in dust

Specific tritium activities, $A_{\text{sp}}(\text{T})$, in dust were determined by FCM enhanced by the heat of Sn oxidation. A histogram in figure 5 shows the amount of T captured in the two bubblers after combusting the JET-C dust collected from the louvres and the outer divertor base. Results are also shown for the remaining amount of T removed by flowing gas through the reactor tube after the combustion, and for T remaining in the ash; the vertical axis is logarithmic. More than 99% of T removed by combustion was captured in the first bubbler. In both samples of dust, the amount of tritium captured in the second bubbler was less than 0.1% that absorbed in the first bubbler. The amounts of T remaining in a reactor tube after FCM and in the ash were four and seven orders of magnitude lower than that in the 1st bubbler, respectively. Tritium leakage from the reactor during the combustion was monitored using an ionisation chamber; no leakage was detected. It clearly shows that the total T content in the specimens could be effectively measured by the enhanced FCM.

Tritium retention data determined by FCM in dust particles from JET-C, ILW-1 and ILW-3 are in figure 6 showing $A_{\text{sp}}(\text{T})$ values and in table 2 where the total activities are also

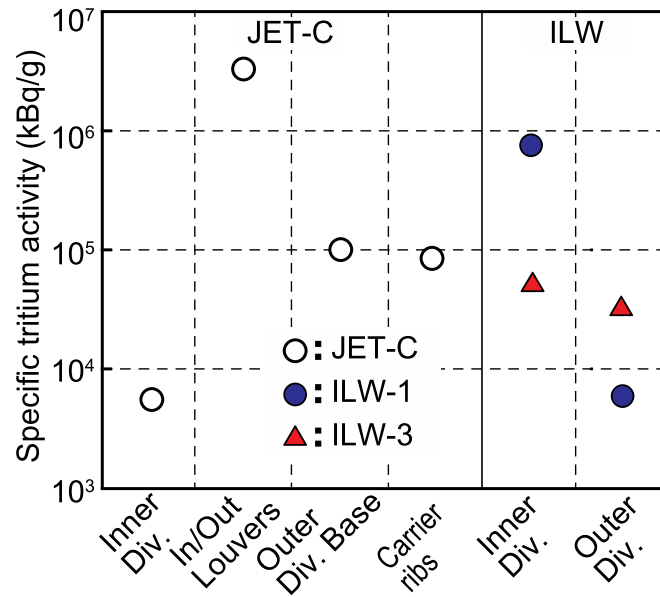


Figure 6. Specific T activities in dust from JET-C, ILW-1 and ILW-3 measured by FCM [7]. Reprinted from [7]. Copyright (2020), with permission from Elsevier.

Table 2. Tritium in dust from JET-C, ILW-1 and ILW-3 measured by FCM.

Campaign	Area	Collected amount (g)	Specific T activity (MBq g ⁻¹)	Total T activity (MBq)
JET-C	Inner divertor	110.1	5	550
	Inner and outer louvers	99.4	2633	261 720
	Outer divertor tiles and base carrier	51.4	106	5448
	Carrier ribs	19.3	70	1351
	Total	280.2		269 069
ILW-1	Inner divertor tiles	0.27	748	202.0
	Outer divertor tiles	0.77	6	4.6
	Total	1.04		206.6
ILW-3	Inner divertor tiles	0.50	55	27.5
	Outer divertor tiles	0.36	36	13.0
	Total	0.86		40.5

calculated taking into account the amount of dust retrieved after respective campaigns. The amounts retrieved after ILW-1 and ILW-3 are over two orders of magnitude smaller than that from JET-C: around 1 g per ILW campaign versus 280 g in JET-C. The specific tritium activities for JET-C and ILW are similar: 5–2600 MBq g⁻¹ for JET-C and 6–750 MBq g⁻¹ after ILW campaigns. At the same time, the total activities differ significantly: 270 GBq after JET-C down to 0.2 GBq after ILW-1 and, only 0.04 GBq after ILW-3. This difference is due to the much lower quantities of dust generated with the metallic wall than in the C surrounding.

The reason for such high specific activity (750 MBq g⁻¹) in the ILW-1 inner divertor sample was identified by detailed examination of individual dust particles. Figure 7(a) shows morphological differences between dust particles on the In disc. The result was obtained by combining SEM images and EPM analysis. The location of C-, Be-, W-dominated dust

particles and also oxygen-rich objects was traced and identified over the whole surface. Very few Be- and W-rich particles were found in comparison to the C-dominated grains thus indicating that the generation rate of metal particles during the ILW operation was insignificant.

Figure 7(b) is the IP-recorded distribution of T intensity on the disc surface. Colours from light blue to red indicate the increasing tritium amount, while the dark blue denotes the surface where T is below the detection limit. Different amounts of T retained in individual dust particles can be inferred. In order to determine which type of particles retain T, the results of elemental EPM analysis, figure 7(a), and tritium distribution, figure 7(b), are super-imposed in figure 7(c). Areas with the T presence are identified and two additional facts are immediately noticed: (i) not all dust particles retain tritium; (ii) T is found at locations where dust particles were not identified with EPMA recorded with the resolution of 20 μm.

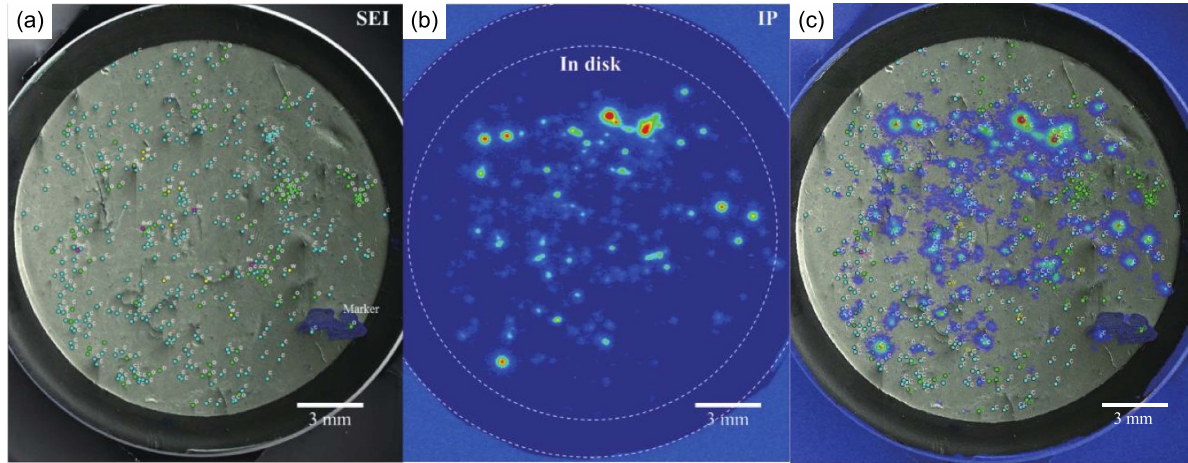


Figure 7. (a) SEM/EPMA image showing the composition of dust particles. Small circles with superscript labels indicate the location and composition (●C: carbon, ●O: oxygen, ●Be: beryllium, and ●W: tungsten) of dust particles. (b) IP image showing tritium distribution on the In disc, (c) imposed image of (a) with (b) [8]. Reprinted from [8], Copyright (2018), with permission from Elsevier.

Over 60% of the C-dominated and around 88% of metal-rich particles do not contain tritium. The presence of particles without T is most likely associated with debris originally located on surfaces remote from the plasma (e.g. C grains released from the bottom of W/CFC tiles during their installation), or strongly heated particles from which fuel was desorbed by direct plasma impact on loose dust or at the tile surface. Elemental analysis also indicates the contamination of dust by aluminium (Al) originating either from the remotely handled robot during in-vessel operations [19] or during sample collection and preparation for analysis. It is stressed again that the number of Be-, W-dominated, and metal oxide dust particles retaining T was very small. In summary, more than 85% of particles retaining tritium were the C-dominated ones. Therefore, it is clearly shown (like in [8, 9]) that T in the ILW dust is mainly associated with the remaining C particles, not with Be and W. The same result was also obtained in studies of deuterium in dust from JET-ILW [20].

3.2. Tritium in divertor tiles

3.2.1. Tritium depth distribution. The ILW-3 tiles were sliced parallel to the surface in order to examine the in-depth tritium distribution. The T amount was measured in all sliced samples. The results are shown in figure 8. On the horizontal axis the thickness of the sliced tiles is given, while $A_{sp}(T)$ values are on the vertical axis. Samples 1–6, 4–10 and 6–2 were sliced about 1 mm from the surface and sample 8–8 was sliced about 0.5 mm from the surface. Most tritium has been found in the topmost surface layer, while only small amounts have been detected in the second and subsequent slices. This demonstrates that the distribution of T in JET divertor samples is concentrated at the surface. The detection of T at the deeper depth is significantly lower than the plasma facing surface and may be related to the diffusion of hydrogen isotopes into CFC [21–23], but also to the contamination of respective samples during sectioning [23] is to be taken into account. At this point

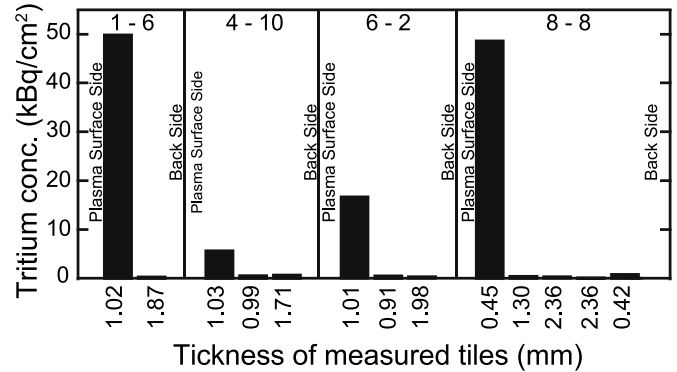


Figure 8. Specific tritium activities determined by FCM in sliced samples from tiles after ILW-3.

it is impossible to address definitely the contribution of the two options. In summary, the results from the sliced samples show that the distribution of T in JET divertor tiles is highly non-uniform with the highest concentrations at the plasma facing surface and significantly lower concentrations in the CFC substrate. This non-uniformity has a direct impact on the assessment of $A_{sp}(T)$ values as differing mass of substrate material can bias the reported value. For this reason the areal activity ($A_a(T)$) is considered for the interpretation of the T activity data presented on divertor samples.

3.2.2. Tritium activity: poloidal distribution. Histograms in figure 9 show the poloidal distribution of $A_a(T)$ determined by FCM in the ILW-1 and ILW-3 samples. The values fluctuate from sample-to-sample but remain within similar ranges for ILW1 and ILW-3: 1–10 kBq cm⁻² (ILW-1) and 0.5–13 kBq cm⁻² (ILW-3). However, the T amounts generated by DD reactions in ILW-1 and ILW-3 were different: respectively around 15 GBq and 40 GBq, as could be inferred from the neutron generation rates in both campaigns. This significant difference by a factor of 2.5 between the campaigns

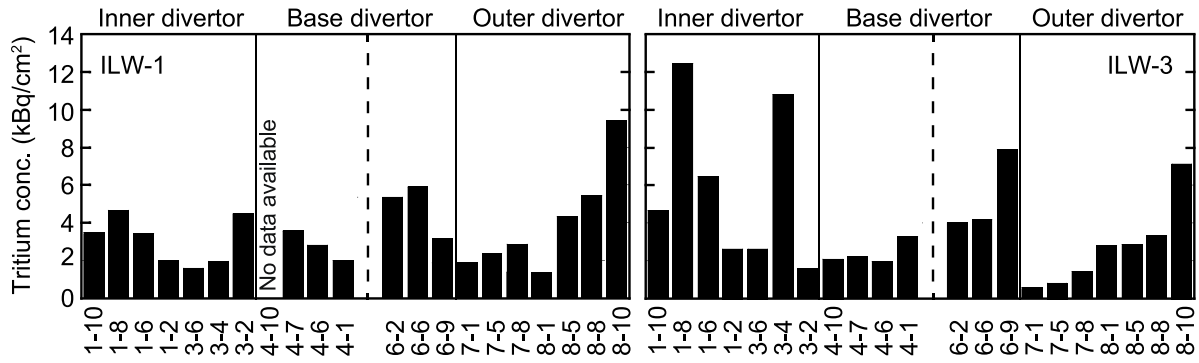


Figure 9. Areal T activities in tiles after ILW-1 and ILW-3 measured by FCM.

is not reflected by the determined $A_a(T)$ values. It may be connected with an additional source of tritium, i.e. off-gas in-vessel from the first deuterium–tritium experiment in JET (DTE1) in 1997 [3, 24]. In-vessel off-gassing cannot be directly quantified though that process might significantly contribute to the results after ILW-1 and ILW-3 if the amount of released tritium exceeded the production of T from DD reaction in the ILW operation. In addition, the inner and outer divertor legs within each operating period are within similar ranges. Such similarities of retention in the two divertor legs were not observed for deuterium (D) measured by nuclear reaction analysis and thermal desorption. The D content was an order of magnitude lower on the outer divertor (tiles 7 and 8) compared with the top of the inner leg (tile 1) [25–27]. The differences in the D and T retention patterns in the divertor point to different mechanisms underlying the retention of both isotopes. Deuterium retention is driven by co-deposition (surface process), while high energy tritons are implanted into the subsurface region. From the SRIM calculation, the maximum ranges of 1 MeV tritons produced by the DD reaction in W and C are about 4 μm and 12 μm , respectively.

3.2.3. Tritium in the surface region. Figure 10 shows results obtained with TIPT for both ILW-1 and ILW-3. The images of cored samples show the tritium distribution on the tiles. The colours reflect the intensity of tritium decay β^- -rays escaping from the depth of a few micrometres, as shown by the reference ‘ART-123’ in the figure. The data reveal that larger amounts of T accumulated on the inner vertical divertor tiles, than on the outer ones, both after ILW-1 and ILW-3. However, the area with noticeable T content is expanded downwards in the ILW-3 case. The intensity is the highest for sample 4–10 (ILW-1) located in the inner divertor inside the pumping duct, i.e. in the region shadowed from the direct plasma line-of-sight. This result can be associated with the presence of tritiated carbon co-deposit, i.e. legacy after JET-C. Other differences in the T distribution on tiles 4 and 6 can be attributed to the different positions of the typical divertor strike points in the two campaigns, as marked in figure 10 with green and blue lines.

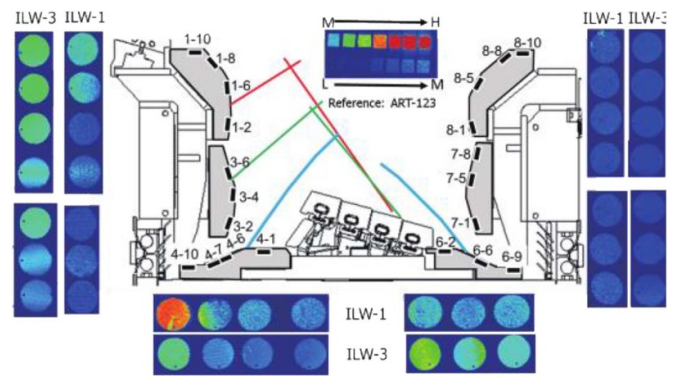


Figure 10. TIPT results of cored samples in ILW-1 and ILW-3, and for a reference T sample. Positions of cored samples are shown in a poloidal cross-section in which left-hand side is the torus inboard side. Coloured lines show the positions of the separatrix in three typical configurations, ILW-1 predominantly green, ILW-2 and 3 green and predominantly blue [6]. Reproduced from [6]. CC BY 4.0.

Histograms in figure 11 show in detail photo-stimulated luminescence (PSL) intensities per unit area and time for x-rays and β^- -rays recorded with TIPT. Sample 6–9 (ILW-3) could not be measured by IP because it was already used for another experiment. Two main features are noticed: (i) greater PSL values (i.e. greater T content) after ILW-3 than after the first campaign; (ii) greater T content in the inner divertor than in the outer one, especially after ILW-3.

The reason for the differences between the T distribution measured by FCM (figure 9) and TIPT (figure 11) is that with FCM one determines T concentration taking into account T in the entire sample, while TIPT measures T distribution at much smaller depth. Torikai *et al* measured the tritium depth profiles of JET Mark IIA type divertor tiles from JET-C by the β^- -ray-induced x-ray spectrometry [28]. The results have shown low T concentration in the very surface layer and high content in the deeper layers. The difference was attributed to the formation of a deposition layer on the surface or the desorption of tritium from the surface due to plasma heating. In summary, TIPT is better for visualisation of tritium distribution, but measurements of the total T amount in tiles should be done by FCM.

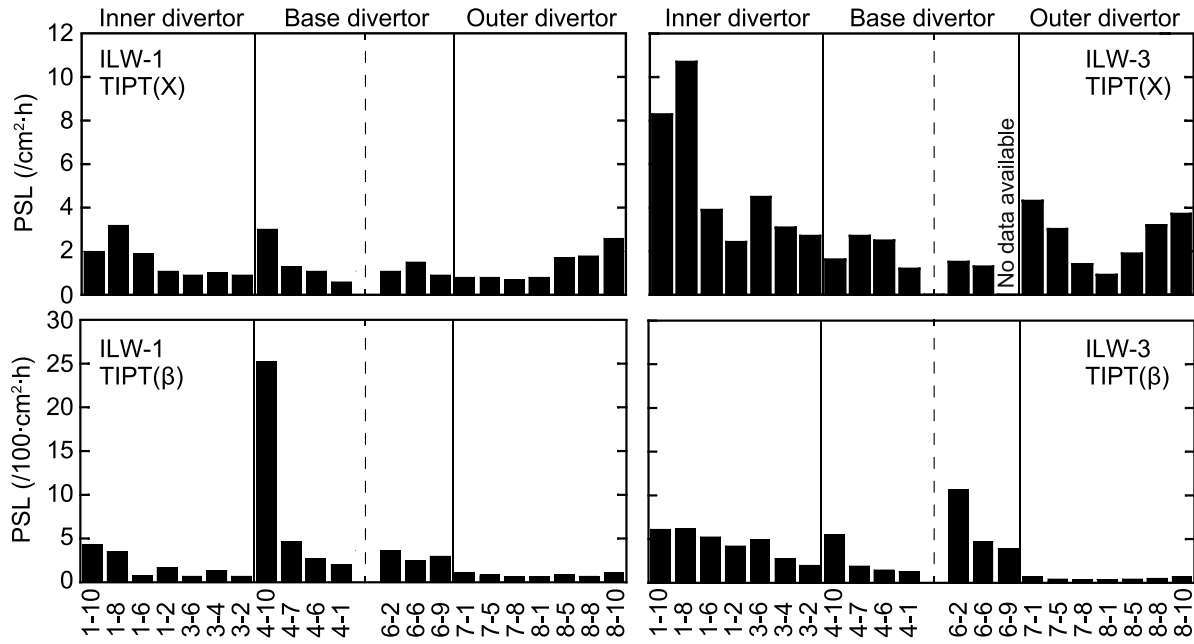


Figure 11. Poloidal distribution of photoluminescence intensities of x-ray and β^- -radiation measured with TIPT for ILW-1 and ILW-3 divertor samples. Note difference in PSL scale between TIPT(X) and TIPT(β) [6]. Reproduced from [6]. CC BY 4.0.

Table 3. Total tritium amount in ILW-1 and ILW-3.

	Tile number	Average T conc. (Bq cm ⁻²)	Surface area (cm ²)	T amount (MBq)	Total number of tiles in vessel (block)	Total T (MBq)	Total T atoms (particle)
ILW-1	1	3395	270	0.92	96	88	$4.94 \times 10^{+16}$
	3	2671	540	1.44	48	69	$3.88 \times 10^{+16}$
	4	2803	320	0.90	96	86	$4.83 \times 10^{+16}$
	6	4809	340	1.64	96	157	$8.81 \times 10^{+16}$
	7	2373	640	1.52	48	73	$4.09 \times 10^{+16}$
	8	5140	350	1.80	96	173	$9.69 \times 10^{+16}$
	Sum			8.22		646	$3.62 \times 10^{+17}$
ILW-3	1	6549	270	1.77	96	170	$9.52 \times 10^{+16}$
	3	5008	540	2.70	48	130	$7.28 \times 10^{+16}$
	4	2381	320	0.76	96	73	$4.10 \times 10^{+16}$
	6	5355	340	1.82	96	175	$9.81 \times 10^{+16}$
	7	928	640	0.59	48	29	$1.60 \times 10^{+16}$
	8	4033	350	1.41	96	136	$7.60 \times 10^{+16}$
	Sum			9.06		713	$3.99 \times 10^{+17}$

4. Discussion

A comparison of $A_{sp}(T)$ in the ILW tiles (figure 8) and dust (figure 6 and table 1) clearly indicates that the values in dust are three to five orders of magnitude greater than those in the tiles. However, it is stressed that the dust collected after the ILW operation is composed to much extent of carbon, therefore the $A_{sp}(T)$ level of dust is similar to that in JET-C. The C dust in ILW is most probably a legacy from the JET-C operation. The crucial result is that the total amount of ILW dust is much smaller than the amount retrieved from JET-C and, the amount of non-carbon dust in ILW dust is even smaller [4, 20]. It clearly indicates that the actual amount of

dust generated in ILW operations is even much smaller than the total of approximately 1 g retrieved by vacuum cleaning. The operation with the metallic wall drastically reduced the dust generation rate and, in a consequence, the total T amount retained in particles was also reduced. Therefore, it is demonstrated that the operation with the JET-ILW (three campaigns, 62 h) led to a significant reduction of dust generation thus effectively reducing the amount and activity of tritiated dust in the reactor.

Table 3 summarises the average T contents in the 2 mm thick samples from the analysed ILW divertor tiles (figure 9). The surface area of each type of tile, the T amount calculated from the surface area and T concentration on each tile, the

number of respective tile in the vacuum vessel, and the total amount of T are given. The T content in most ILW tiles is about 1 MB, while 3 MBq is the maximum value. From the T amount in each tile and the number of respective tiles in the JET vacuum vessel, the T content in the divertor after ILW-1 and ILW-3 campaigns could be assessed at the level of 713 MBq and 646 MBq, respectively. The generated T amounts by DD reactions in ILW-1 and ILW-3 were approximately 15 GBq and 40 GBq. Therefore, the amounts based on the FCM results correspond to 4.8% and 1.6% of the total T generation in ILW-1 and ILW-3 operations, respectively. These values are higher than the deuterium retention determined after ILW-1 and ILW-3: 0.2% of the injected deuterium fuel [25, 27]. This may be due to the implantation of 1 MeV tritons from DD reaction. However, if an additional off-gassing source of T from DTE1 is taken into account the actual T retention rate in ILW could be lower.

5. Concluding remarks

The main contribution of this work to fuel retention studies is the integrated approach to tritium determination in dust and divertor tiles after three distinct periods of JET operation. Due to the use of full combustion and imaging techniques it could be shown that the T presence in dust collected from JET-ILW is predominantly connected with carbon particles being a legacy after the JET-C operation, while the retention in Be- and W-based particles is minor. Radiography and FCMs have also provided a comprehensive picture on the amount and distribution of T in the divertor tiles. This has facilitated a comparison between the T retention and the total T generation in DD reactions during respective campaigns. The quantification of T inventories of divertor samples by full combustion reveal similar areal activities at the inner and outer divertor legs. This is a result of implantation of 1 MeV tritons as the main retention mechanism. Finally, the development of research methodology and gathered laboratory experience will be crucial in future studies of materials retrieved after full D–T campaigns in fusion devices.

Acknowledgments

This work was carried out within the framework of the Broader Approach DEMO R&D Activity and the EUROfusion Consortium, funded by the European Union via the Euratom Research and Training Programme (Grant Agreement No 101052200—EUROfusion). Views and opinions expressed are however those of the author(s) only and do not necessarily reflect those of the European Union or the European Commission. Neither the European Union nor EAN Commission can be held responsible for them. The work has been supported by the Swedish Research Council (VR) (Grants 2015–04844 and 2016–05380) and the UK EPSRC Energy Programme (Grant Number EP/W006839/1). This work was performed with the support and under the auspices of the NIFS Collaboration Research Program (NIFS21KLPF082).

ORCID iDs

S. Masuzaki  <https://orcid.org/0000-0003-0161-0938>
M. Tokitani  <https://orcid.org/0000-0002-3744-2481>
Y. Hatano  <https://orcid.org/0000-0001-5084-5931>
A. Widdowson  <https://orcid.org/0000-0002-6805-8853>
M. Rubel  <https://orcid.org/0000-0001-9901-6296>

References

- [1] Matthews G.F. 2013 Plasma operation with an all metal first wall: comparison of an ITER-like wall with carbon wall in JET *J. Nucl. Mater.* **438** S2–10
- [2] Merola M., Escourbiac F., Raffray R., Chappuis P., Hirai T. and Martin A. 2014 Overview and status of ITER internal components *Fusion Eng. Des.* **89** 890–5
- [3] Coad P., Rubel M., Likonen J., Bekris N., Brezinsek S., Matthews G.F., Mayer M. and Widdowson A.M. 2018 Migration and retention studies during the JET carbon divertor campaigns *Fusion Eng. Des.* **138** 78–108
- [4] Rubel M. et al 2018 Dust generation in tokamaks: overview of beryllium and tungsten dust characterisation in JET with the ITER-like wall *Fusion Eng. Des.* **136** 579–86
- [5] Hatano Y. et al 2019 Tritium distribution on W-coated divertor tiles used in the third ITER-like wall campaign *Nucl. Mater. Energy* **18** 258–61
- [6] Lee S.E. et al 2021 Global distribution of tritium in JET with the ITER-like wall *Nucl. Mater. Energy* **26** 100930
- [7] Ashikawa N. et al 2020 Determination of retained tritium from ILW dust particles in JET *Nucl. Mater. Energy* **22** 100673
- [8] Otsuka T. et al 2018 Tritium retention characteristics in dust particles in JET with ITER-like wall *Nucl. Mater. Energy* **17** 279–83
- [9] Widdowson A. et al 2013 Comparison of JET main chamber erosion with dust collected in the divertor *J. Nucl. Mater.* **438** S827–32
- [10] De Temmerman G. et al 2021 Data on erosion and hydrogen fuel retention in beryllium plasma-facing materials *Nucl. Mater. Energy* **27** 100994
- [11] Tanabe T. 2017 *Tritium: Fuel of Fusion Reactors* (Springer)
- [12] Jespersen D., Hyslop A. and Brady J.E. 2014 *Chemistry: The Molecular Nature of Matter* (Wiley)
- [13] Sato T. et al 2018 Features of particle and heavy ion transport code system (PHITS) version 3.02 *J. Nucl. Sci. Technol.* **55** 684–90
- [14] Katz L. and Penhold A.S. 1952 Range-energy relations for electrons and the determination of beta-ray end-point energies by absorption *Rev. Mod. Phys.* **24** 28
- [15] Asakura N. et al 2013 Investigation of carbon dust accumulation in the JT-60U tokamak vacuum vessel *J. Nucl. Mater.* **438** S659–63
- [16] Otsuka T. and Tanabe T. 2017 Application of a tritium imaging plate technique to depth profiling of hydrogen in metals and determination of hydrogen diffusion coefficients *Mater. Trans.* **58** 1364–72
- [17] Otsuka T. and Hatano Y. 2016 Tritium retention in individual metallic dust particles examined by a tritium imaging plate technique *Phys. Scr.* **2016** 014010
- [18] Schindelin J. et al 2012 FIJI: an open-source platform for biological-image analysis *Nat. Methods* **9** 676–82
- [19] Rubel M., Widdowson A., Fortuna-Zalesna E., Ayres C., Berry M., Burford M., Collins S. and Macheta P. 2020 Search for mobilized dust during operations with equipment for remote handling in JET with ITER-like wall *Phys. Scr.* **2020** 014048

- [20] Fazinic S., Božičević-Mihali I., Provatas G., Tadić T., Rubel M., Fortuna-Zalešna E. and Widdowson A. 2020 Micro-analyses of dust particles generated in JET tokamak with the ITER-like wall *Nucl. Fusion* **60** 136031
- [21] Penzhorn R.D., Bekris N., Berndt U., Coad J.P., Ziegler H. and Nägele W. 2001 Tritium depth profiles in graphite and carbon fibre composite material exposed to tokamak plasmas *J. Nucl. Mater.* **288** 170
- [22] Rubel M., Emmoth B., Bergsker H., Wienhold P., Dunaev V. and Sukhomlinov V. 1992 Deposition and in-depth penetration of deuterium in carbon fibre composites *J. Nucl. Mater.* **196–198** 285
- [23] Emmoth B., Rubel M. and Franconi E. 1990 Deep penetration of deuterium in carbon based substrates exposed to the PISCES plasma *Nucl. Fusion* **30** 1140
- [24] Keilhacker M. *et al* 1999 High fusion performance from deuterium-tritium plasmas in JET *Nucl. Fusion* **39** 209
- [25] Heinola K. *et al* 2016 Long-term fuel retention in JET ITER-like wall *Phys. Scr.* **2016** 014075
- [26] Krat S. *et al* 2020 Comparison of erosion and deposition in JET divertor during the first three ITER-like wall campaigns *Phys. Scr.* **2020** 014059
- [27] Widdowson A. *et al* 2021 Evaluation of tritium retention in plasma facing components during JET tritium operations *Phys. Scr.* **96** 124075
- [28] Torikai Y., Matsuyama M., Bekris N., Glugla M., Coad P., Naegele W., Erbe A., Noda N., Philipps V. and Watanabe K. 2005 Tritium distribution in JET Mark IIA type divertor tiles analysed by BIXS *J. Nucl. Mater.* **337–339** 575–9